Multicomponent Transport of Alcohols in an Anion Exchange Membrane Measured by *In-Situ* ATR FTIR Spectroscopy

Blaine M. Carter,[1] Breanna M. Dobyns,[2] Bryan S. Beckingham,[2] and Daniel J. Miller[1]*

*Corresponding Author, Tel: +1 (510) 495-2353 E-mail: danieljmiller@lbl.gov

[1]Joint Center for Artificial Photosynthesis, Lawrence Berkeley National Laboratory, Berkeley, CA 97420, United States

[2]Department of Chemical Engineering, Auburn University, Auburn, AL 36849, United States

Abstract

Multicomponent transport through membranes is encountered in many applications, including photoelectrochemical CO_2 reduction devices that convert CO_2 into alcohols. We report the use of *in-situ* ATR FTIR spectroscopy to quantify the permeability of Selemion AMV, a commonly used anion exchange membrane, to mixtures of alcohols. An i*n-situ* ATR FTIR spectrophotometer probe inserted into a standard diffusion cell enabled straightforward measurement of membrane permeability in multicomponent transport experiments without the need to periodically remove aliquots from the diffusion cell. The solubilities of alcohols in Selemion AMV were measured using a standard desorption technique. The solution-diffusion model was used to calculate alcohol diffusivities in Selemion AMV from measured permeabilities and solubilities. The relative contributions of alcohol solubility and diffusivity to overall permeability are discussed, and changes in permeability, solubility, and diffusivity with changing composition in binary and ternary alcohol mixtures are described.

Keywords

Permeability, multicomponent transport, in-situ ATR FTIR spectroscopy

1. Introduction

Photoelectrochemical reduction of CO_2 could provide a renewable avenue to chemical feedstocks and carbon-neutral liquid transportation fuels. CO_2 reduction to high-value products could reduce worldwide dependence on finite fossil fuel resources and mitigate the effects of greenhouse gas emissions. Carbon dioxide reduction products, including carbon monoxide, methane, ethylene, and various small alcohols have been reported on copper and copper containing alloys [1]. Alcohols (*e.g.*, methanol, ethanol, propanol) are liquid fuels that could be distributed using existing infrastructure and burned in internal combustion engines. If CO_2 used to produce the alcohols were sustainably captured from the atmosphere or from exhaust that would otherwise be emitted to the atmosphere, combustion of these alcohols would be an overall carbon-neutral process.

Photoelectrochemical CO_2 reduction devices typically consist of two electrodes, an aqueous electrolyte, and a polymeric membrane separating the electrode compartments [2,3]. Water is oxidized to O_2 at the anode and CO_2 is reduced to an alcohol (or other product) at the cathode. The membrane must permit the transport of electrolyte ions so current can flow from one electrode to the other, but it also must block the transport of CO_2 reduction products dissolved in the aqueous electrolyte. If CO_2 reduction products easily migrate from the cathode to the anode, they will be re-oxidized and overall device efficiency will decrease [4]. One drawback of presently-known CO_2 reduction catalysts is that they generally lack selectivity (*i.e.*,

they simultaneously reduce CO_2 to several different products, rather than to a single product). Therefore, the membrane must effectively control the transport of multiple CO_2 reduction products.

Membranes used in CO_2 reduction devices (and in many energy generation and storage applications employing an aqueous electrolyte) are often comprised of polyelectrolytes [5]. These membranes contain charged moieties covalently bound to the polymer backbone or side chains. Due to the strong affinity of polar water molecules for the fixed charge groups attached to the polymer chains, these membranes are often highly hydrated and can swell substantially in water or aqueous electrolyte [6]. Though highly swollen, these membranes are non-porous and transport of water molecules, ions, and other small molecule species is described by the solution-diffusion model [7]. According to this model, transport of an ion or neutral molecule through a dense polymer film consists of three steps: (1) sorption into the polymer at one film face, (2) diffusion through the film thickness, and (3) desorption from the polymer on the opposing film face [6]. The overall permeability, P_i, of polymer to solute *i* is therefore the product of the solute solubility, K_i, and diffusivity, D_i, in the polymer:

$$P_i = D_i K_i \tag{1}$$

The permeability of a membrane to a solute in the liquid phase is often measured in a diffusion cell, where the membrane is positioned between a donor chamber, containing a solution of relatively high concentration, and a receiver chamber, containing a solution of relatively low concentration (*e.g.*, ultrapure water) [8]. Permeation of the solute from the donor chamber to the receiver chamber is motivated by the difference in its chemical potential between the solution of high concentration and the solution of low concentration [7]. To calculate the permeability of the membrane to a solute, the concentration of the solute in the receiver chamber is measured as

a function of time. The time-resolved concentration data are then fit to a model describing solute permeation through hydrated films [8,9].

It is often desirable to measure the simultaneous transport of multiple solutes through a membrane, since membranes are often challenged in practice with separating complex mixtures [10–12]. Phenomena such as flux coupling [13] and competitive sorption [14] can influence the transport of solutes in mixtures. The transport of gas mixtures is demonstrably different than the transport of individual gases, especially in the presence of gases that induce high levels of plasticization (*e.g.*, CO_2) in glassy polymers [15]. In sulfonated polymers, which are of interest for desalination and other applications, the transport of monovalent ions is affected by the presence of divalent ions [16,17]. These phenomena are not always well understood or easily predicted *a priori*; therefore, the measurement of multicomponent transport in polymeric materials is of considerable interest.

Quantitative characterization of multicomponent transport through membranes is challenging. Measurement of the transport of multiple gaseous species across a membrane film requires periodic detection by gas chromatography in a mixed gas permeation system [15]. In the liquid phase, methods employed to monitor solute concentration in a diffusion cell are often not suitable for solute mixtures. Conductivity is frequently employed to measure membrane permeability to an ionic solute (*e.g.*, sodium chloride [16]) and total organic carbon analysis has been used in the case of small organic molecules (*e.g.*, methanol [17]), but these techniques are not capable of distinguishing among solutes in mixtures. Techniques capable of independently measuring the concentration of multiple solutes, such as gas chromatography or liquid chromatography, require periodic sampling [18], which can be labor-intensive and, if the aliquots are of sufficient volume, can complicate permeability calculations.

Herein, we employ *in-situ* attenuated total reflectance Fourier transform infrared (ATR FTIR) spectroscopy to determine the permeability of a membrane to mixtures of methanol, ethanol, and *n*-propanol using a simple diffusion cell. The concentration of each alcohol in the receiver chamber of a diffusion cell was monitored by automatically collecting solution IR spectra via an *in-situ* ATR FTIR probe inserted into the receiver chamber. Using molar absorptivities obtained by calibrating the instrument with standard alcohol solutions, absorbance spectra were deconvoluted and the resultant time-resolved concentration data were fit to a model to extract the membrane permeability to each alcohol. The solubility of each alcohol in the membrane was determined by a desorption technique [19]. From the measured permeability and solubility, the diffusivity of each alcohol in the membrane was calculated from Equation (1).

ATR FTIR spectroscopy has previously been used to characterize transport in polymer systems. The diffusion coefficients of solvents as they evaporated out of polymer solutions cast onto an ATR crystal were measured by Karimi [20]. The diffusion coefficient of water in an epoxy resin [21] and in polyacrylonitrile [22] was measured by contacting a film mounted on an ATR crystal with liquid water. Sammon, Breen, and co-workers extended this experimental concept to measuring the sorption and diffusion of water and acetone mixtures in poly(vinyl alcohol) and poly(vinyl alcohol)/clay nanocomposites [22–24]. Fu and Lim measured the diffusion of multicomponent mixtures of several organic solutes into linear low-density polyethylene films by contacting one side of a film for a specified time, and then quickly pressing the film on a crystal and taking an ATR FTIR spectrogram. A deconvolution treatment was used to isolate the contributions of each solute to the spectra [25]. In each of these studies, the polymer film was placed directly on the ATR crystal and the infrared absorbance of the polymer/solute pair was measured to quantify solubility and/or diffusivity of the solute(s) in the

film. In this study, ATR FTIR spectroscopy is used to measure the concentration of solutes in the receiver chamber solution after they pass through a membrane film mounted in a standard diffusion cell, permitting calculation of overall membrane permeability. In addition to enabling calculation of overall membrane permeability, this technique ensures full hydration of the membrane film throughout the entire experimental duration. Hydration of a polymer film strongly affects the diffusion of solutes within it [6]. Hallinan and Elabd measured the permeability of Nafion® 117 to methanol in a diffusion cell using ATR FTIR spectroscopy to monitor the receiver chamber methanol concentration However, in their study, the receiver chamber solution was circulated to a standard benchtop ATR FTIR spectrometer [26–29] (rather than being measured directly as was the case in this study), and the permeation of mixtures with other solutes was not measured.

For this study, the membrane selected was Selemion AMV, an anion exchange membrane based on a blend of poly(vinyl chloride) and polystyrene that contains quaternary ammonium fixed charge groups [30,31]. Selemion AMV has been employed in several studies of CO_2 reduction catalysis [32–34]. In a CO_2 reduction device, a supporting electrolyte (*e.g.*, K_2CO_3/$KHCO_3$) is typically employed, so the majority of the charge carriers are carbonate and bicarbonate anions. Therefore, anion exchange membranes are generally preferred over cation exchange membranes in CO_2 reduction devices, since electrolyte anions are electrostatically repelled from a cation exchange membrane. Devices employing a cation exchange membrane can experience very high polarization losses, even at low current densities, relative to systems employing an anion exchange membrane [2].

2. Materials and Methods

2.1 Materials

Selemion AMV was purchased from AGC Engineering Co., Ltd. (Chiba, Japan). The membranes were stored in a cool, dry place, and kept hydrated at all times. Samples were cut from a sheet using a 35 mm hammer-driven steel hole punch. Samples were immersed in fresh ultrapure water for at least 24 hours before use. Ultrapure water was supplied by an EMD Millipore Milli-Q Integral 3 water purification system (18.2 MΩ•cm at 25 °C, 1.2 ppb TOC) (Billerica, MA). Methanol, ethanol, and *n*-propanol (reagent grade, ≥ 99.5% purity) were purchased from Sigma-Aldrich (St. Louis, MO) and used as received.

2.2 Calibration with Standard Solutions

Solution infrared absorbance was measured using a Mettler-Toledo ReactIR™ 15 *in-situ* ATR FTIR spectrophotometer with a shallow tip 9.5 mm DSub AgX DiComp probe. Data were collected using iC IR 4.3 software. Infrared absorbance spectra consisting of 256 averaged scans were collected over a range of wavenumbers: 650 cm^{-1} – 2500 cm^{-1}. The instrument response was first calibrated to obtain effective molar absorptivities using standard solutions of methanol, ethanol, and *n*-propanol carefully prepared at several concentrations in the range 0.01 – 1.0 M. The instrument probe was first immersed in ultrapure water to obtain a background spectrum, which was subtracted from all subsequent spectra. The probe was then dried and immersed in a calibration solution. The absorbance at key wavenumbers was measured as the height of peaks to a two-point baseline established between 932 cm^{-1} and 1182 cm^{-1}. The probe was cleaned with ultrapure water and dried before moving onto the next calibration solution. To validate the use of *in-situ* ATR FTIR spectroscopy for determination of solution concentration in alcohol

mixtures, several binary and ternary solutions were prepared in equimolar and non-equimolar proportions. The absorbance of these solutions was measured and concentrations of constituent alcohols were determined using the effective molar absorptivities determined from the calibration solutions. Concentrations determined in this way were compared to actual solution concentrations.

2.3 Alcohol Permeation Experiments

Permeation experiments were carried out using a standard diffusion cell (Adams and Chittenden Scientific Glassware, Berkeley, CA). Each half-cell had a volume of 35 mL, a 3/8" sampling port at the top, and a vertical ground glass face with a 15 mm orifice. The fully hydrated membrane was sandwiched between two silicone gaskets (also with a 15 mm orifice in their centers) and clamped between the two half cells. The half cells were jacketed, and water was circulated through the jackets to maintain the solution temperature at 25 °C throughout each experiment. One of the two identical half cells (the receiver chamber) was filled with 30 mL of ultrapure water. The other half cell (the donor chamber) was filled with enough ultrapure water such that, when the required volume of alcohol was added to the cell, the total solution volume would be 30 mL. The *in-situ* ATR FTIR probe was inserted into the receiver chamber, ensuring that the probe tip was fully wetted. An ultrapure water spectrum was taken as a background spectrum, and this background spectrum was subtracted from all subsequent spectra. After the ultrapure water background spectrum was captured, enough alcohol (methanol, ethanol, and/or *n*-propanol) was added to the donor chamber such that the concentration of each alcohol in the resultant solution was 1.0 M. The infrared absorbance of the receiver chamber in the range 650 cm^{-1} – 2500 cm^{-1} was recorded at one minute intervals for approximately 24 hours. The

absorbance at key wavenumbers was measured as the height of peaks to a two-point baseline established between 932 cm^{-1} and 1182 cm^{-1}. After the conclusion of the permeation experiment, a digital caliper was used to measure the film thickness. A photo of the experimental setup is shown in Figure 1.

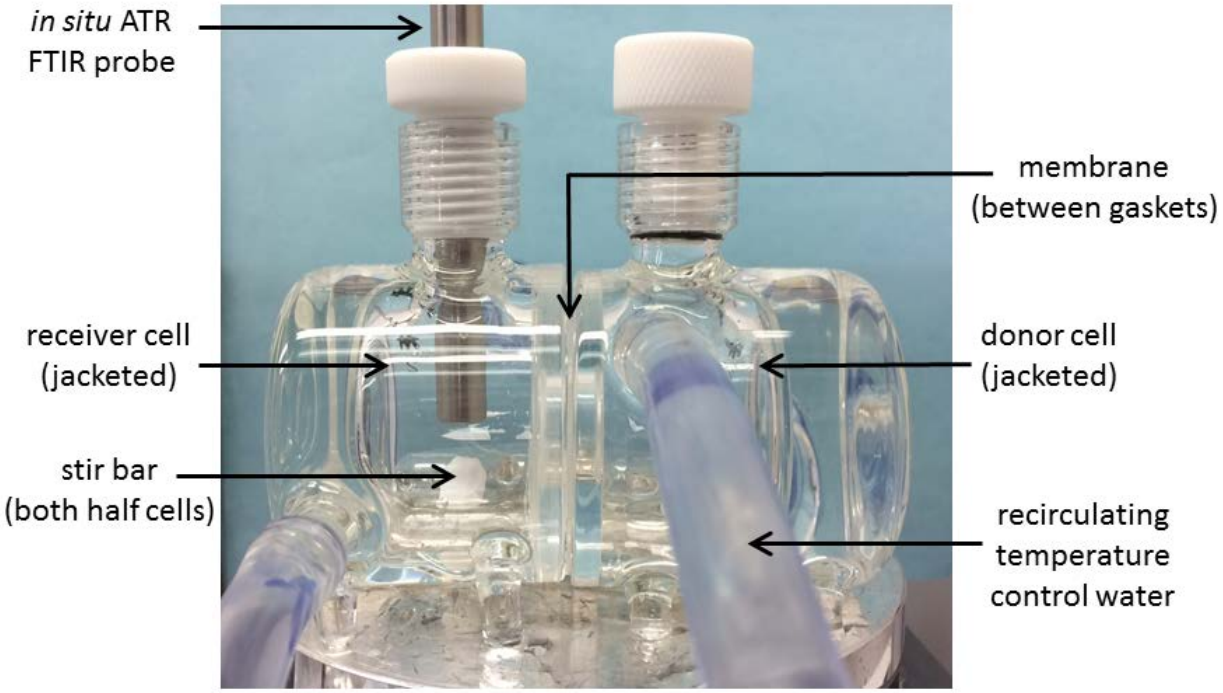

Figure 1. Photograph of experimental setup. The membrane is clamped between halves of the jacketed diffusion cell, with the *in-situ* ATR FTIR probe inserted into the receiver chamber.

2.4 Alcohol Sorption Experiments

Desorption experiments [19] were used to measure methanol, ethanol, and *n*-propanol solubility in Selemion AMV. Hydrated membrane samples were quickly patted dry and immersed in *ca*. 30 mL of an alcohol solution (1.0 M in methanol, ethanol, *n*-propanol, and mixtures thereof). Membranes were soaked for three days, after which time samples were

removed from the soaking solution and quickly blotted dry. The thickness and diameter of the samples were quickly measured using a caliper before immersing each sample in a precisely known volume (*ca*. 15 mL) of ultrapure water in a clean jar. (The exact water volume was calculated by metering the water into a jar on a mass balance and converting the water mass to volume by its density). The samples were soaked in the ultrapure water for 72 hours, allowing any sorbed alcohol to migrate from the membrane into the external solution. The concentration of methanol, ethanol, and/or *n*-propanol in the desorption solution was measured using a Thermo Fisher (Waltham, MA) Ultimate 3000 UHPLC system with an ERC RefractoMax 520 refractive index detector and a VWD-3100 Variable Wavelength UV detector. The samples were then blotted dry and immersed in precisely known volume of fresh ultrapure water (*ca*. 15 mL) in a clean jar. After soaking for 72 hours, the concentration of methanol, ethanol, and *n*-propanol in the second desorption solution was measured. No alcohol was detected in the second desorption solution, suggesting that all of the sorbed alcohol had migrated out of the membrane sample during the first desorption step. The solubility (or sorption coefficient) of a solute *i* in the polymer was calculated as [19]:

$$K_i = \frac{c_i^m}{c_i^s} \tag{2}$$

where c_i^m is the solute concentration in the membrane and c_i^s is the solute concentration (1.0 M) in the external solution. The concentration of solute in the membrane c_i^m was be calculated from the volume of the swollen membrane, the volume of the desorption solution, and the measured concentration of solute in the desorption solution.

3. Results and Discussion

3.1 Effective Molar Absorptivities of Alcohols

The concentration, *c*, of an absorbing species in solution is related the absorbance of the solution, A_λ, at any given wavenumber, λ, by the Beer-Lambert law [35]:

$$A_\lambda = \log\left(\frac{I_0}{I}\right) = E_\lambda l c \tag{3}$$

where I_0 and I are the intensities of incident and transmitted light, respectively, E_λ is the molar absorptivity of the absorbing species, and l is the path length. In this study, the path length of the transmitted light was identical in all measurements, so an effective molar absorptivity (ε_{eff}) is defined as $\varepsilon_\lambda = E_\lambda l$, yielding:

$$A_\lambda = \varepsilon_\lambda c \tag{4}$$

The choice of wavenumbers for absorbance measurement was guided by the absorbance spectra of methanol, ethanol, and *n*-propanol (Figure 2). Several peaks were identified where one or more of the alcohols absorb strongly, including those at λ = 962 cm^{-1}, 1007 cm^{-1}, 1018 cm^{-1}, 1044 cm^{-1}, 1070 cm^{-1}, and 1089 cm^{-1}.

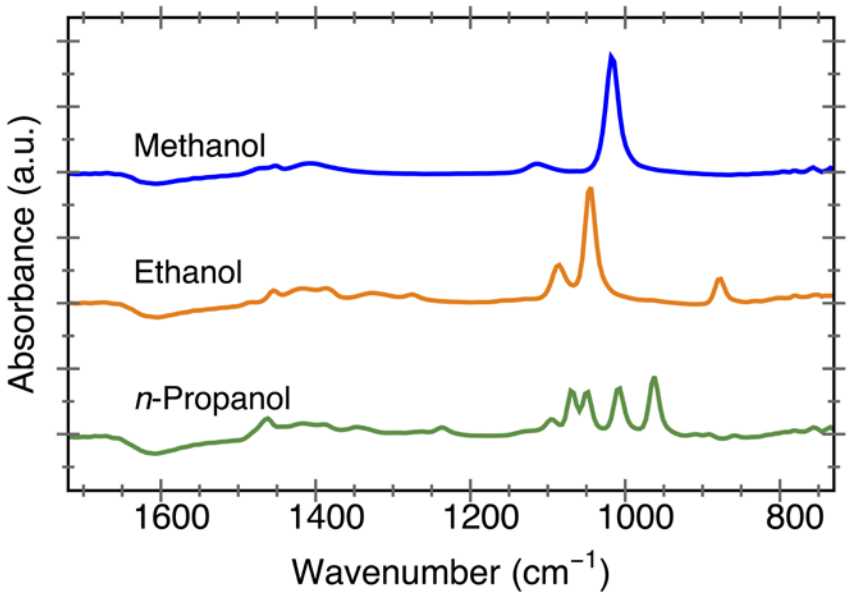

Figure 2. ATR FTIR spectra of 1.0 M solutions of (—) methanol, (—) ethanol, and (—) *n*-propanol between 750 cm^{-1} and 1700 cm^{-1}. Spectra are offset for clarity.

To use the absorbance at each of these wavenumbers in the measurement of alcohol solution concentration, the effective molar absorptivity (ε_λ) of each of the alcohols was determined for each wavenumber. The absorbance of carefully prepared standard solutions of methanol, ethanol, and *n*-propanol was measured at each of the aforementioned wavenumbers over the concentration range 0.01 M – 1.0 M. This concentration range was chosen because the donor solution in permeation experiments (described later) was 1.0 M in each alcohol. Several measurements were made in the low concentration range (0.01M – 0.2M), as the evolving concentration of alcohol in the receiver chamber was generally in this range during the experimental timeframe (approximately 24 hours for each measurement). Linear regressions were made over the absorbance of standard solutions, measured as a function of concentration (Figure 3) at each wavenumber of interest.

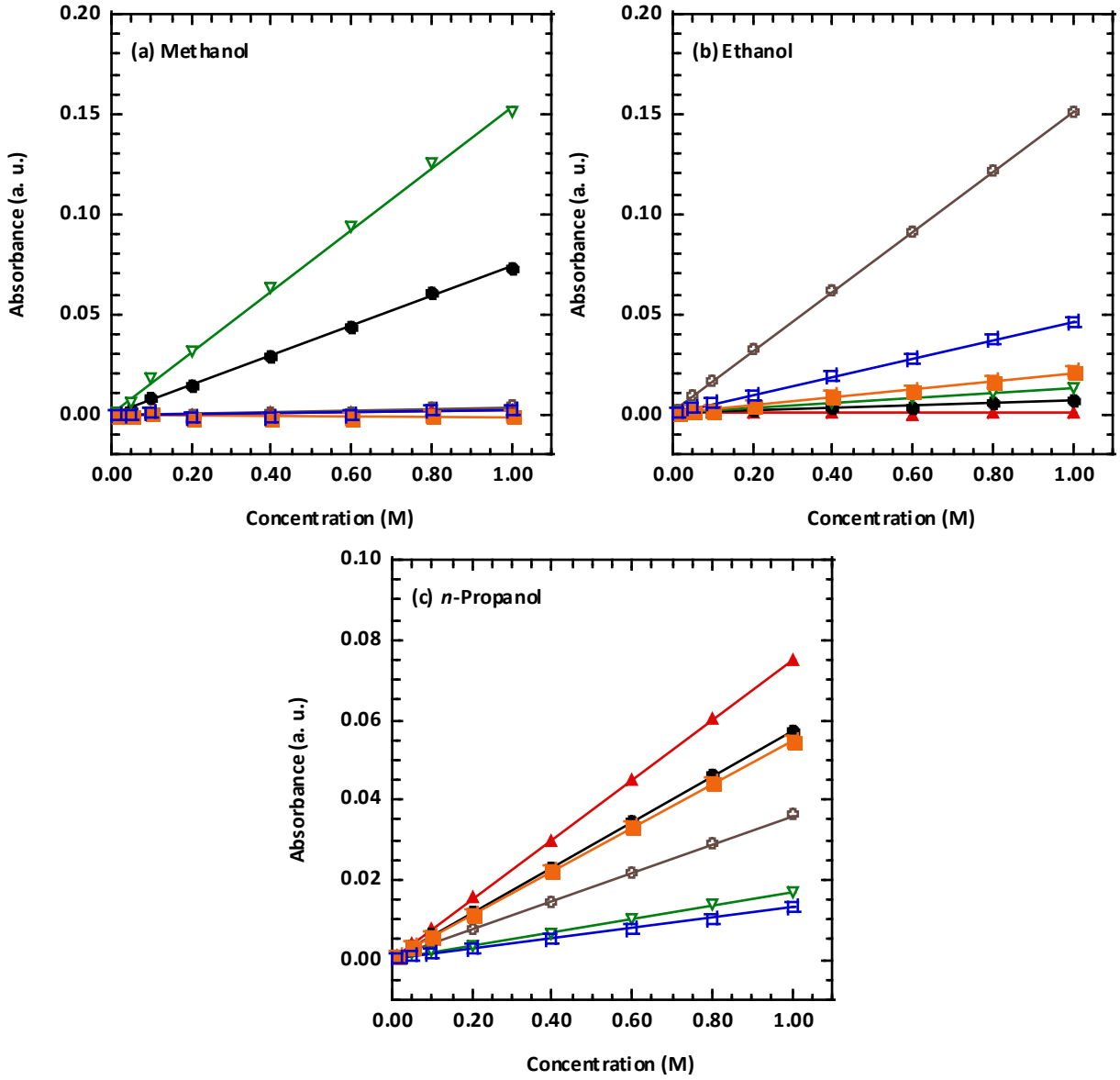

Figure 3. ATR FTIR absorbance as a function of a) methanol, b) ethanol, and c) *n*-propanol concentration (M) in ultrapure water at wavenumbers (▲) 962 cm^{-1}, (●) 1007 cm^{-1}, (▽) 1018 cm^{-1}, (○) 1044 cm^{-1}, (■) 1070 cm^{-1}, (□) 1089 cm^{-1}. Lines are linear best-fits to absorbance data, measured as height from a two-point baseline between 932 cm^{-1} and 1182 cm^{-1}.

The effective molar absorptivity (ε_i) for each alcohol at each wavenumber is the slope of the linear regressions shown in Figure 3. These values are tabulated in Table 1, along with their respective squared correlation coefficients (R^2). In two cases, (ethanol at 962 cm^{-1} and methanol

at 1070 cm^{-1}), a linear fit to absorbance data that passed through the origin could not be achieved (and, therefore, no squared correlation coefficient is reported) due to insignificant absorbance, so the molar absorptivity of these alcohols was taken as zero at these wavenumbers.

Table 1: Effective molar absorptivities and their squared correlation coefficients.

	Methanol		**Ethanol**		***n*-Propanol**	
λ [cm^{-1}]	ε_λ	R^2	ε_λ	R^2	ε_λ	R^2
962	0.0017	0.8951	0.0000	--	0.0751	0.9998
1007	0.0741	0.9992	0.0067	0.9750	0.0576	0.9995
1018	0.1540	0.9988	0.0135	0.9929	0.0171	0.9965
1044	0.0037	0.7762	0.1522	0.9994	0.0363	0.9991
1070	0.0000	--	0.0211	0.996	0.0553	0.9995
1089	0.0013	0.2309	0.0461	0.9993	0.131	0.9974

3.2 Measurement of Concentrations in Alcohol Mixtures

For a solution containing multiple solutes with known molar absorptivities (ε_{ij}), the Beer-Lambert law can be extended to include the contributions of each solute *i* to the total absorbance A_j at wavenumber *j*:

$$A_j = \sum_{i,j=1}^{n} \varepsilon_{ij} c_i \tag{5}$$

The concentration c_i of *n* solutes was determined by measuring the absorbance A_j at *n* wavenumbers. For two solutes *A* and *B*, a system of two independent equations may be written for wavenumbers *1* and *2*:

$$\left.\begin{aligned} A_1 &= \varepsilon_{A1} c_A + \varepsilon_{B1} c_B \\ A_2 &= \varepsilon_{A2} c_A + \varepsilon_{B2} c_B \end{aligned}\right\} \tag{6}$$

Similarly, for three solutes *A*, *B*, and *C*, a system of three independent equations may be written for wavenumbers *1*, *2*, and *3*:

$$\left.\begin{aligned} A_1 &= \varepsilon_{A1}C_A + \varepsilon_{B1}C_B + \varepsilon_{C1}C_C \\ A_2 &= \varepsilon_{A2}C_A + \varepsilon_{B2}C_B + \varepsilon_{C2}C_C \\ A_3 &= \varepsilon_{A3}C_A + \varepsilon_{B3}C_B + \varepsilon_{C3}C_C \end{aligned}\right\} \quad (7)$$

To validate the use of *in-situ* ATR FTIR spectroscopy for accurate measurement of alcohol concentration in a mixture, several binary and ternary alcohol solutions were carefully prepared. The absorbance of the solutions was measured by *in-situ* ATR FTIR spectroscopy and the concentrations of the constituent alcohols were calculated using the effective molar absorptivities determined from the calibrations (Table 1) and either Equation System (6) (for binary solutions) or Equation System (7) (for ternary solutions). The three wavenumbers chosen for absorbance measurement were 962 cm^{-1}, 1018 cm^{-1}, and 1044 cm^{-1}. At each of these wavenumbers, one of the alcohols exhibited the greatest absorbance (and, consequently, had the greatest molar absorptivity): methanol at 1018 cm^{-1} (ε_λ = 0.1540), ethanol at 1044 cm^{-1} (ε_λ = 0.1522), and *n*-propanol at 962 cm^{-1} (ε_λ = 0.0751).

Figure 4 shows a comparison between measured and actual concentrations of methanol and ethanol in binary solutions. Methanol and ethanol concentrations were 0.05 M, 0.075 M, 0.10 M, 0.125 M, and 0.15 M in equimolar and non-equimolar solutions. Concentrations were calculated by simultaneously solving the Equation System (6) using the effective molar absorptivities of methanol and ethanol at 1018 cm^{-1} and 1044 cm^{-1}. The identity line ($y = x$) is shown, representing perfect agreement between the measured and actual solution concentrations. Proximity to the identity line indicates the accuracy of the measurement. Overall, agreement between measured and actual concentration is very good, with some deviation at 0.05 M (20%

error in methanol and 15% error in ethanol). At higher concentrations, error was generally 5% or less.

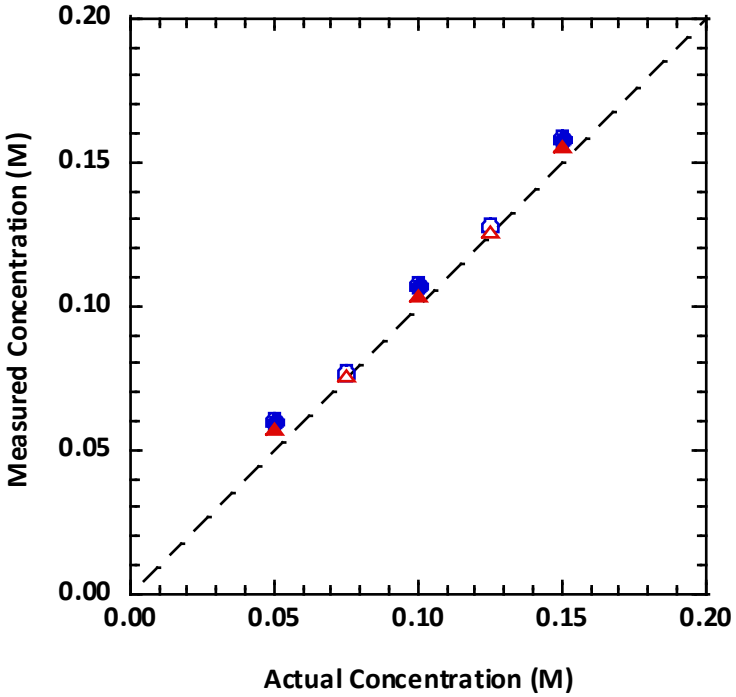

Figure 4. Comparison of concentration (M) calculated from ATR FTIR absorbance at 1018 cm^{-1} and 1044 cm^{-1} and prepared solution concentration (M) for binary solutions of (●) methanol and (▲) ethanol. Filled symbols denote equimolar solutions (*i.e.* [methanol]:[ethanol] of [0.05 M]:[0.05 M], [0.10 M]:[0.10 M], and [0.15 M]:[0.15 M]), and open symbols denote non-equimolar solutions (*i.e*. [methanol]:[ethanol] of [0.075 M]:[0.125 M] and [0.125 M]:[0.075 M]). The dotted line is the identity line ($y = x$), which represents perfect agreement between measured concentration and actual concentration.

Figure 5 compares the measured and actual concentrations of methanol and *n*-propanol in binary solutions. Concentrations were calculated by simultaneously solving Equation System (6) using the effective molar absorptivities of methanol and *n*-propanol at 962 cm^{-1} and 1018 cm^{-1}. Again, the measured methanol concentration was about 20% higher than the actual solution concentration at 0.05 M, but methanol measurements at higher concentrations had errors of 7% or less. The largest deviation in measured *n*-propanol concentration occurred at 0.075 M (16%),

but measurements at other *n*-propanol concentrations displayed excellent accuracy (3% error or less).

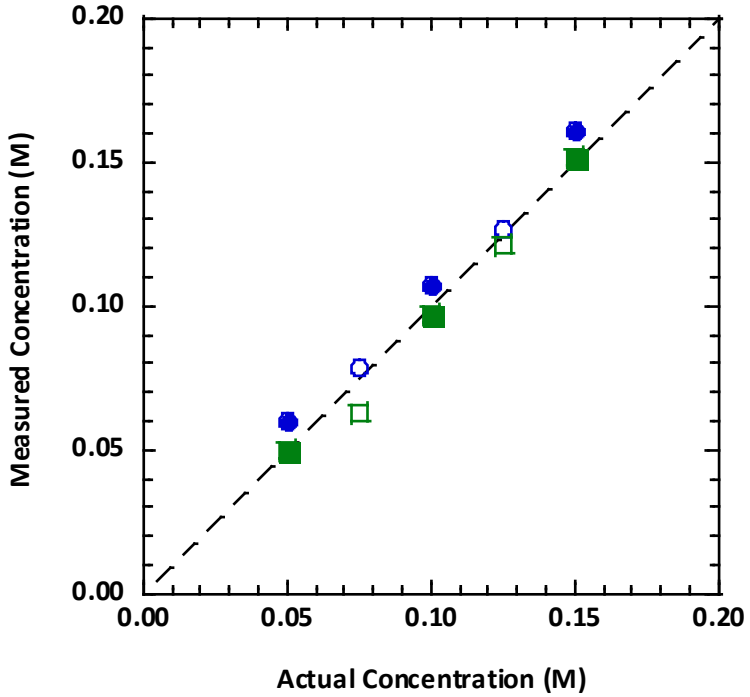

Figure 5. Comparison of concentration (M) calculated from ATR FTIR absorbance at 962 cm^{-1} and 1018 cm^{-1} and prepared solution concentration (M) for binary solutions of (●) methanol and (■) *n*-propanol. Filled symbols denote equimolar solutions (*i.e.* [methanol]:[*n*-propanol] of [0.05 M]:[0.05 M], [0.10 M]:[0.10 M], and [0.15 M]:[0.15 M]), and open symbols denote non-equimolar solutions (*i.e.* [methanol]:[*n*-propanol] of [0.075 M]:[0.125 M] and [0.125 M]:[0.075 M]). The dotted line is the identity line ($y = x$), which represents perfect agreement between measured concentration and actual concentration.

Measured and actual concentrations of ethanol and *n*-propanol in binary solution are compared in Figure 6. Concentrations were calculated using the effective molar absorptivities of ethanol and *n*-propanol at 962 cm^{-1} and 1044 cm^{-1}. Ethanol exhibited essentially no absorbance at 962 cm^{-1} (*cf.*, Table 1), so the concentration of *n*-propanol was calculated directly with Equation (4) and the absorbance at 962 cm^{-1}. The calculated concentration of ethanol was about 14% higher than the actual concentration at 0.05 M, but the error at higher concentrations was

3% or less. Generally, the error in calculated *n*-propanol concentrations was approximately 10% or less.

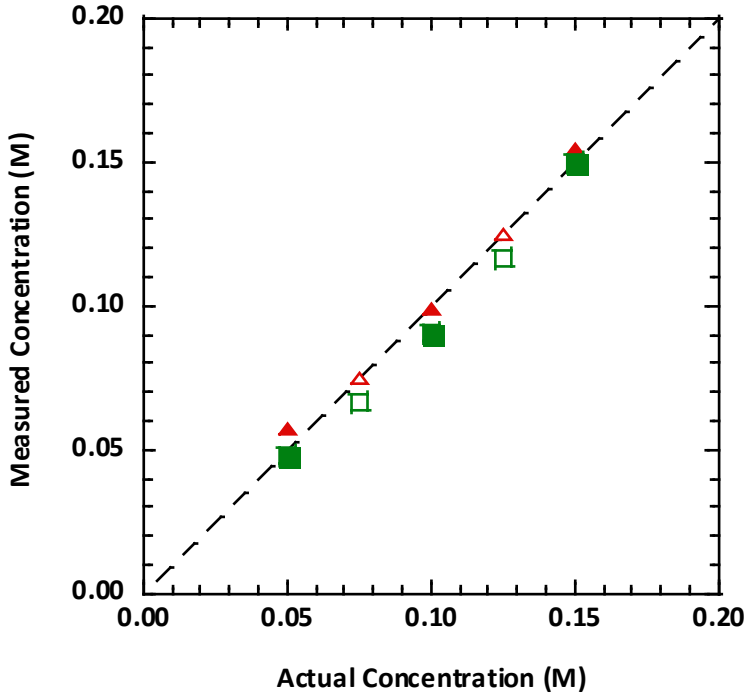

Figure 6. Comparison of concentration (M) calculated from ATR FTIR absorbance at 962 cm^{-1} and 1044 cm^{-1} and prepared solution concentration (M) for binary solutions of (▲)ethanol and (■) *n*-propanol. Filled symbols denote equimolar solutions (*i.e.* [ethanol]:[*n*-propanol] of [0.05 M]:[0.05 M], [0.10 M]:[0.10 M], and [0.15 M]:[0.15 M]), and open symbols denote non-equimolar solutions (*i.e.* [ethanol]:[*n*-propanol] of [0.075 M]:[0.125 M] and [0.125 M]:[0.075 M]). The dotted line is the identity line ($y = x$), which represents perfect agreement between measured concentration and actual concentration.

A comparison of measured and actual concentrations of methanol, ethanol, and *n*-propanol in ternary solutions is shown in Figure 7. Three equimolar solutions were prepared, with each of the alcohols in concentrations of 0.05 M, 0.10 M, and 0.15 M. Using their effective molar absorptivities at 962 cm^{-1}, 1018 cm^{-1}, and 1044 cm^{-1}, alcohol concentrations were calculated by simultaneously solving the three equations in Equation System (7). The error on measured methanol concentration was 5% or less at all concentrations. The agreement between

measured and actual ethanol concentration was excellent, with an error of only 1% at all three concentrations. The most significant deviation in measured concentration was for *n*-propanol at 0.05 M, where a 14% error was observed. However, at 0.10 M and 0.15 M, the error was only 7% and 6%, respectively.

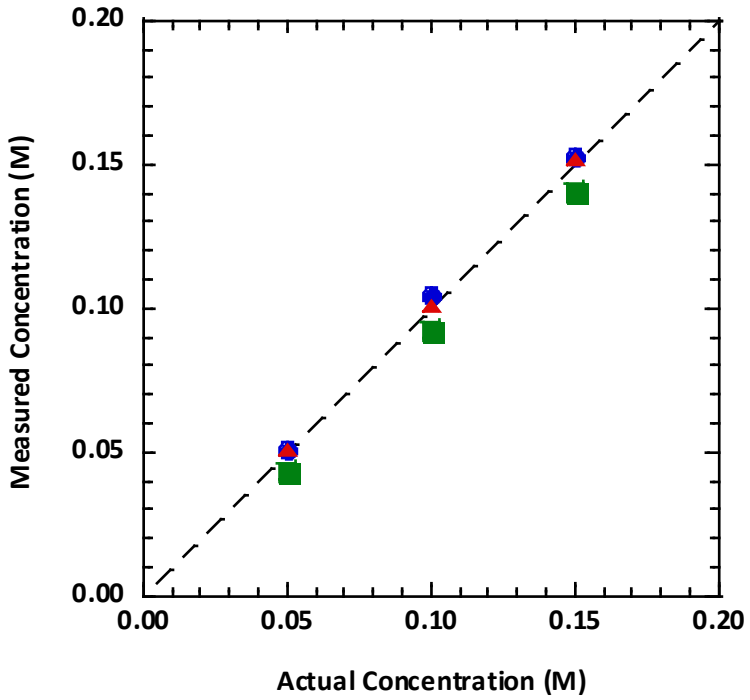

Figure 7. Comparison of concentration (M) calculated from ATR FTIR absorbance at 962 cm^{-1}, 1018 cm^{-1}, and 1044 cm^{-1} and prepared solution concentration (M) for ternary solutions of (●) methanol, (▲)ethanol, and (■) *n*-propanol. All solutions were equimolar: 0.05 M, 0.10 M, and 0.15 M in all three solutes. The dotted line is the identity line ($y = x$), which represents perfect agreement between measured concentration and actual concentration.

Generally, the accuracy of the concentrations obtained from in-situ ATR FTIR spectroscopy measurements was satisfactory. Even the largest observed error of 20% in methanol concentration in binary solutions at 0.05 M (Figures 4 and 5) is not large in absolute terms. An error of 20% on a measurement at 0.05 M is indicative of a resolution of 0.01 M or better, two orders of magnitude smaller than the donor chamber concentration (1.0 M) and at least an order of magnitude lower than typical receiver chamber concentrations in permeability

experiments. Over all of the binary and ternary solutions measured in this study, the average error was 6% for methanol concentration, 3% for ethanol concentration, and 6% for *n*-propanol concentration. All measured concentrations for the binary and ternary solutions shown in Figures 4-7 as well as the error of each measurement are tabulated in the Supporting Information.

3.3 Transport of Alcohols in Selemion AMV

We have established that *in-situ* ATR FTIR spectroscopy may be used to accurately measure the concentration of mixed alcohols in solution. We will now apply this measurement technique to the characterization of alcohol transport across a Selemion AMV polyelectrolyte membrane. An *in-situ* ATR FTIR probe inserted into the receiver chamber of a standard diffusion cell (Figure 1) enabled the periodic, automatic sampling of the receiver chamber solution absorbance. The concentration of an alcohol in the receiver chamber solution was directly calculated from each absorbance measurement using Equation (4) in the case of single component transport, or using Equation System (6) or (7) in the case of multicomponent transport.

Yasuda *et al*. developed a model that describes the time dependent transport of salts and organic molecules through hydrated polymer films [8,9,36]:

$$\ln\left(1 - 2\frac{c_{it}}{c_{i0}}\right) = P_i\left(-\frac{2A}{Vl}t\right) \tag{8}$$

where P_i is the membrane permeability to solute i, A is the membrane area available for transport (1.767 cm^2), V is the volume of solution in the donor and receiver chambers (30 mL), l is the membrane thickness, c_{it} is the solute concentration at time t in the receiver chamber, and c_{i0} is the initial solute concentration in the donor chamber (1.0 M). This model has previously been used

to calculate the permeability of hydrogels [16], desalination materials [37], and dialysis membranes [36] to various solutes. The membrane permeability may be extracted by fitting this model to time-resolved receiver chamber concentration data using the permeability as an adjustable parameter. Figure 8 shows measured concentrations of methanol, ethanol, and n-propanol in the receiver chamber during a permeation experiment from a ternary alcohol solution. Lines are fits of the Yasuda model to the concentration data.

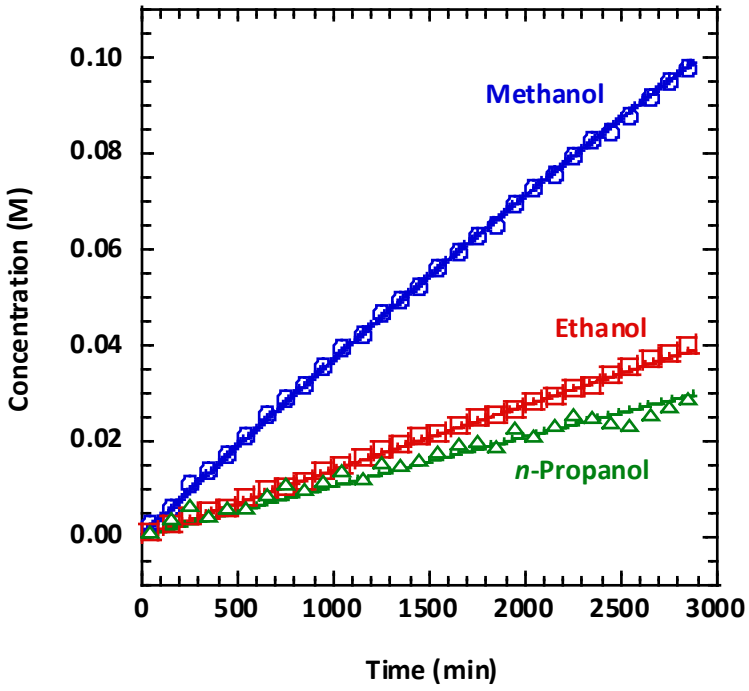

Figure 8. Measured concentrations of methanol, ethanol, and n-propanol in the receiver chamber during a permeation experiment with a ternary mixture of 1.0 M methanol, 1.0M ethanol, and 1.0 M n-propanol in the donor chamber. Lines are fits of the Yasuda model to concentration data. Concentration was recorded once per minute; for clarity, only 1% of concentration data are shown.

The calculated diffusive permeability of Selemion AMV to methanol, ethanol, and *n*-propanol are shown in Table 2, including permeabilities from unary, binary, and ternary alcohol solutions. Tabulated values are averages of three replicate measurements (on different

membrane samples), and uncertainties are standard deviations on the three replicate measurements. The permeability of Selemion AMV to methanol (1.4×10^{-7} cm^2/s) was about three times that to ethanol (4.0×10^{-8} cm^2/s), and the permeability to ethanol was about twice that to *n*-propanol (2.4×10^{-8} cm^2/s). The measured permeability to methanol slightly decreased when methanol was co-permeating with ethanol and/or *n*-propanol, although these values are not statistically distinct from the permeability to methanol alone. The permeability to ethanol in a binary mixture with methanol was identical to the permeability to ethanol alone. The permeability to ethanol exhibited a slight, but not statistically significant, increase when co-permeating with *n*-propanol or as a ternary mixture with methanol and *n*-propanol. The permeability to *n*-propanol alone was statistically the same as the permeability to n-propanol in binary mixtures with methanol or ethanol. The maximum permeability to *n*-propanol was from a ternary solution with methanol and ethanol, where the measured permeability was about 40% higher than the permeability to *n*-propanol alone.

Table 2. Diffusive permeabilities of methanol, ethanol, *n*-propanol, and mixtures thereof in Selemion AMV. For ternary mixtures, co-solutes were: (a) ethanol and *n*-propanol, (b) methanol and *n*-propanol, (c) methanol and ethanol. Uncertainties are standard deviations on three replicate measurements.

Alcohol Diffusive Permeabilities (cm^2/s) in Selemion AMV			
	Methanol	**Ethanol**	***n*-Propanol**
Single Solute	$(1.4 \pm 0.3) \times 10^{-7}$	$(4.0 \pm 0.6) \times 10^{-8}$	$(2.4 \pm 0.8) \times 10^{-8}$
Binary Mixture with Methanol	--	$(4.0 \pm 0.4) \times 10^{-8}$	$(2.2 \pm 0.9) \times 10^{-8}$
Binary Mixture with Ethanol	$(1.14 \pm 0.06) \times 10^{-7}$	--	$(2.9 \pm 0.5) \times 10^{-8}$
Binary Mixture with n-Propanol	$(1.0 \pm 0.1) \times 10^{-7}$	$(4.1 \pm 0.2) \times 10^{-8}$	--
Ternary Mixture	$(1.15 \pm 0.05) \times 10^{-7(a)}$	$(4.2 \pm 0.1) \times 10^{-8(b)}$	$(3.4 \pm 0.1) \times 10^{-8(c)}$

The transport of ions and organic molecules in a dense, non-porous polymer film is described by the solution-diffusion model (Equation (1)), which gives the permeability as the product of the solute solubility and diffusivity in the polymer. Therefore, independent measurement of the solute solubility and/or diffusivity in the polymer can provide a more

detailed description of overall transport. The solubility is the partitioning of a solute from an external solution into the membrane polymer. The partitioning of methanol, ethanol, and *n*-propanol in Selemion AMV from unary, binary, and ternary mixtures are reported in Table 3. The solubility is the ratio of alcohol concentration inside the membrane to the concentration in the external solution. In this study, the concentration of each alcohol in the external solution was 1.0 M, so the reported solubilities indicate the molar concentration of each alcohol in the membrane polymer.

Methanol and *n*-propanol exhibited similar solubilities in Selemion AMV (0.26 and 0.27, respectively). The solubility of ethanol in Selemion AMV (0.125) was about half that of methanol and *n*-propanol. Therefore, the uptake of methanol and *n*-propanol was more favorable than the uptake of ethanol. Alcohol solubilities in Selemion AMV were only slightly affected by the presence of other alcohols, and suggest that some weak competitive effects could influence alcohol uptake from binary or ternary external solutions. For example, the solubility of methanol in a binary mixture with ethanol was higher than its solubility in a binary mixture with *n*-propanol. This result is likely due to the more favorable uptake of methanol than ethanol. The solubility of ethanol slightly decreased in binary and ternary mixtures with methanol and/or *n*-propanol relative to the uptake of ethanol alone. This result could be indicative of a competitive sorption phenomenon that weakly favors methanol or *n*-propanol over ethanol uptake. Within the experimental errors calculated, the uptake of *n*-propanol was invariant with solution composition.

Table 3. Solubilities of methanol, ethanol, *n*-propanol, and mixtures thereof in Selemion AMV. For ternary mixtures, co-solutes are: (a) ethanol and *n*-propanol, (b) methanol and *n*-propanol, (c) methanol and ethanol. Uncertainties are standard deviations on three replicate measurements.

Alcohol Solubilities in Selemion AMV			
	Methanol	**Ethanol**	***n*-Propanol**
Single Solute	0.26 ± 0.03	0.125 ± 0.009	0.27 ± 0.03
Binary Mixture with Methanol	--	0.12 ± 0.01	0.26 ± 0.02
Binary Mixture with Ethanol	0.29 ± 0.01	--	0.256 ± 0.007
Binary Mixture with n-Propanol	0.26 ± 0.03	0.108 ± 0.007	--
Ternary Mixture	0.27 ± 0.01[(a)]	0.110 ± 0.008[(b)]	0.25 ± 0.01[(c)]

As permeability is the product of solubility and diffusivity of a solute in a polymer film (Equation (1)), solute diffusivities may be calculated directly from measured permeabilities (Table 2) and measured solubilities (Table 3). Calculated diffusivities for methanol, ethanol, and *n*-propanol in unary, binary, and ternary mixtures are shown in Table 4. The diffusivity of methanol was the highest (5×10^{-7} cm^2/s). The diffusivity of ethanol (3.2×10^{-7} cm^2/s) was lower than that of methanol. The lowest diffusivity was exhibited by *n*-propanol (9×10^{-8} cm^2/s). Solute diffusivity is inversely proportional to solute size [6]. Methanol is the smallest of the alcohols studied here, with a dimeter of 3.6 Å, while ethanol has a diameter of 4.5 Å and *n*-propanol has a diameter of 4.7 Å [38]. The small size of a methanol molecule enabled rapid diffusion among free volume elements in the membrane polymer. Methanol diffusivities in binary and ternary mixtures with ethanol and/or *n*-propanol may have weakly decreased relative to the diffusivity exhibited by methanol alone, although the calculated standard deviations suggest that the diffusivity of methanol varied little with the addition of ethanol and *n*-propanol. Similarly, the diffusivities of ethanol and *n*-propanol may have increased in binary and ternary mixtures relative to the diffusivities exhibited for these alcohols alone, although calculated standard deviations suggest that differences, if any, are slight. These results could be indicative of weak coupled fluxes, which have been shown to affect solute diffusivities in desalination

materials [39]. Coupled fluxes, which are the result of molecular friction among diffusing solute molecules, can either increase or decrease diffusivities, unexpectedly enhancing or depressing diffusion coefficients. Here, the presence of fast-diffusing methanol could slightly enhance the diffusion of ethanol and *n*-propanol. Conversely, slow-diffusing ethanol and *n*-propanol could slightly depress the diffusion of methanol.

Table 4. Diffusivities of methanol, ethanol, *n*-propanol, and mixtures thereof in Selemion AMV, calculated from permeabilities (Table 1) and solubilities (Table 2). For ternary mixtures, co-solutes are: (a) ethanol and *n*-propanol, (b) methanol and *n*-propanol, (c) methanol and ethanol. Uncertainties are propagated (as described by Harris [40]) from the uncertainties reported for permeabilities and solubilities.

Solute Diffusivities (cm^2/s) in Selemion AMV			
	Methanol	**Ethanol**	***n*-Propanol**
Single Solute	$(5 \pm 1) \times 10^{-7}$	$(3.2 \pm 0.5) \times 10^{-7}$	$(9 \pm 3) \times 10^{-8}$
Binary Mixture with Methanol	--	$(3.3 \pm 0.5) \times 10^{-7}$	$(9 \pm 4) \times 10^{-8}$
Binary Mixture with Ethanol	$(4.0 \pm 0.4) \times 10^{-7}$	--	$(1.1 \pm 0.2) \times 10^{-7}$
Binary Mixture with n-Propanol	$(4.0 \pm 0.8) \times 10^{-7}$	$(3.8 \pm 0.3) \times 10^{-7}$	--
Ternary Mixture	$(4.4 \pm 0.5) \times 10^{-7(a)}$	$(4.2 \pm 0.7) \times 10^{-7(b)}$	$(1.15 \pm 0.03) \times 10^{-7(c)}$

With values for permeability (Table 2), solubility (Table 3), and diffusivity (Table 4), we can examine the relative contributions of solubility and diffusivity to overall permeability within the context of the solution-diffusion model (Equation (1)). Methanol had the highest solubility and diffusivity of the three alcohols studied. The high permeability of methanol relative to ethanol and *n*-propanol is, therefore, the product of both high solubility and high diffusivity in Selemion AMV. The solubility and diffusivity of ethanol in Selemion AMV were lower than those of methanol, both of which contribute to an overall lower permeability. The solubility of *n*-propanol in Selemion AMV was higher than that of ethanol and similar to that of methanol; however, the lower diffusivity of the large *n*-propanol molecule contributed to a lower overall permeability to *n*-propanol than to either methanol or ethanol.

4. Conclusions

In this study, we have demonstrated that in-situ ATR FTIR spectroscopy is an accurate tool for measurement of alcohol concentration in unary, binary, and ternary solutions. We subsequently showed that *in-situ* ATR FTIR spectroscopy can be used to monitor the evolving solute concentration in the receiver chamber of a standard diffusion cell during a permeation experiment, enabling measurement of multicomponent alcohol permeation through dense, hydrated membranes. Controlling alcohol transport through hydrated membranes is a key challenge in several electrochemical applications, including solar fuels devices, where a multiplicity of CO_2 reduction products may be produced by non-selective metallic catalysts. Coupling multicomponent alcohol permeation experiments with alcohol sorption experiments permitted the calculation of alcohol diffusivities in the membrane. Alcohol solubility and diffusivity contributed to overall trends in permeability in accordance with the solution-diffusion model. Weak competitive sorption and flux coupling phenomena may have contributed to slight variations in alcohol solubility and diffusivity in multicomponent mixtures.

5. Acknowledgments

This material is based upon work performed at the Joint Center for Artificial Photosynthesis, a DOE Energy Innovation Hub, supported through the Office of Science of the U.S. Department of Energy under Award Number DE-SC000493. This work was also supported by the California Energy Commission (CEC) under contract 500-11-23. BSB gratefully acknowledges start-up funds provided by the Department of Chemical Engineering and the College of Engineering at Auburn University. BMD appreciates a Woltosz Fellowship awarded by the Auburn University College of Engineering. BMD and BSB greatly appreciate financial

support provided the US National Science Foundation through the Auburn University Integrative Graduate Research and Education Traineeship (IGERT) program (Award# 1069004).

6. References

[1] K.P. Kuhl, E.R. Cave, D.N. Abram, T.F. Jaramillo, New insights into the electrochemical reduction of carbon dioxide on metallic copper surfaces, Energy Environ. Sci. 5 (2012) 7050. doi:10.1039/c2ee21234j.

[2] M.R. Singh, E.L. Clark, A.T. Bell, Effects of Electrolyte, Catalyst, and Membrane Composition and Operating Conditions on the Performance of Solar-Driven Electrochemical Reduction of Carbon Dioxide, Phys. Chem. Chem. Phys. 17 (2015) 18924–18936. doi:10.1039/C5CP03283K.

[3] M.R. Singh, A.T. Bell, Design of an artificial photosynthetic system for production of alcohols in high concentration from CO2, Energy Environ. Sci. 9 (2016) 193–199. doi:10.1039/C5EE02783G.

[4] A. Berger, R.A. Segalman, J. Newman, Material requirements for membrane separators in a water-splitting photoelectrochemical cell, Energy Environ. Sci. 7 (2014) 1468–1476. doi:10.1039/c3ee43807d.

[5] J. Kamcev, B.D. Freeman, Charged Polymer Membranes for Environmental/Energy Applications, Annu. Rev. Chem. Biomol. Eng. 7 (2016) 111–133. doi:10.1146/annurev-chembioeng-080615-033533.

[6] G.M. Geise, D.R. Paul, B.D. Freeman, Fundamental water and salt transport properties of polymeric materials, Prog. Polym. Sci. 39 (2013) 1–42. doi:10.1016/j.progpolymsci.2013.07.001.

[7] J.G. Wijmans, R.W. Baker, The solution-diffusion model: a review, J. Memb. Sci. 107 (1995) 1–21. doi:10.1016/0376-7388(95)00102-I.

[8] H. Yasuda, C.E. Lamaze, L.D. Ikenberry, Permeability of Solutes through Hydrated Polymer Membranes. Part I. Diffusion of Sodium Chloride, Makromol. Chemie. 118 (1968) 19–35. doi:10.1002/macp.1968.021180102.

[9] H. Yasuda, L.D. Ikenberry, C.E. Lamaze, Permeability of Solutes through Hydrated Polymer Membranes. Part II. Permeability of Water Soluble Organic Solutes, Makromol. Chemie. 125 (1969) 108–118. doi:10.1002/macp.1969.021250111.

[10] K.C. O'Brien, W.J. Koros, T.A. Barbari, E.S. Sanders, A new technique for the measurement of multicomponent gas transport through polymeric films, J. Memb. Sci. 29 (1986) 229–238. doi:10.1016/S0376-7388(00)81262-4.

[11] D.R. Paul, Reformulation of the solution-diffusion theory of reverse osmosis, J. Memb. Sci. 241 (2004) 371–386. doi:10.1016/j.memsci.2004.05.026.

[12] S. Postel, S. Wessel, T. Keil, P. Eiselt, M. Wessling, Multicomponent mass transport in organic solvent nanofiltration with solvent mixtures, J. Memb. Sci. 466 (2014) 361–369. doi:10.1016/j.memsci.2014.04.017.

[13] W.M. Deen, Analysis of Transport Phenomena, Oxford University Press, New York, NY, 1998.

[14] C.A. Scholes, S.E. Kentish, G.W. Stevens, Effects of Minor Components in Carbon Dioxide Capture Using Polymeric Gas Separation Membranes, Sep. Purif. Rev. 38 (2009) 1–44. doi:10.1080/15422110802411442.

[15] K.L. Gleason, Z.P. Smith, Q. Liu, D.R. Paul, B.D. Freeman, Pure- and mixed-gas permeation of CO2 and CH4 in thermally rearranged polymers based on 3,3'-dihydroxy-4,4'-diamino-biphenyl (HAB) and 2,2'-bis-(3,4-dicarboxyphenyl) hexafluoropropane dianhydride (6FDA), J. Memb. Sci. 475 (2015) 204–214. doi:10.1016/j.memsci.2014.10.014.

[16] H. Ju, A.C. Sagle, B.D. Freeman, J.I. Mardel, A.J. Hill, Characterization of sodium chloride and water transport in crosslinked poly(ethylene oxide) hydrogels, J. Memb. Sci. 358 (2010) 131–141. doi:10.1016/j.memsci.2010.04.035.

[17] M. Galizia, D.R. Paul, B.D. Freeman, Liquid methanol sorption, diffusion and permeation in charged and uncharged polymers, Polymer. 102 (2016) 281–291. doi:10.1016/j.polymer.2016.09.010.

[18] P. McCormick, J. Pellegrino, F. Mantovani, G. Sarti, Water, salt, and ethanol diffusion through membranes for water recovery by forward (direct) osmosis processes, J. Memb. Sci. 325 (2008) 467–478. doi:10.1016/j.memsci.2008.08.011.

[19] G.M. Geise, L.P. Falcon, B.D. Freeman, D.R. Paul, Sodium chloride sorption in sulfonated polymers for membrane applications, J. Memb. Sci. 423–424 (2012) 195–208. doi:10.1016/j.memsci.2012.08.014.

[20] M. Karimi, A.A. Tashvigh, F. Asadi, F.Z. Ashtiani, Determination of concentration-dependent diffusion coefficient of seven solvents in polystyrene systems using FTIR-ATR technique: experimental and mathematical studies, RSC Adv. 6 (2016) 9013–9022. doi:10.1039/C5RA25244J.

[21] P. Wu, H.W. Siesler, Water diffusion into epoxy resin: A 2D correlation ATR-FTIR investigation, Chem. Phys. Lett. 374 (2003) 74–78. doi:10.1016/S0009-2614(03)00691-2.

[22] A.F. Breen, C. Breen, F. Clegg, L.-M. Döppers, Khairuddin, M. Labet, et al., FTIR-ATR studies of the sorption and diffusion of acetone:water mixtures in poly(vinyl alcohol)-clay nanocomposites, Polymer. 53 (2012) 4420–4428. doi:10.1016/j.polymer.2012.07.057.

[23] L.M. Döppers, C. Breen, C. Sammon, Diffusion of water and acetone into poly(vinyl alcohol)-clay nanocomposites using ATR-FTIR, Vib. Spectrosc. 35 (2004) 27–32. doi:10.1016/j.vibspec.2003.11.008.

[24] L.-M. Döppers, C. Sammon, C. Breen, J. Yarwood, FTIR-ATR studies of the sorption and diffusion of acetone/water mixtures in poly(vinyl alcohol), Polymer. 47 (2006) 2714–2722. doi:10.1016/j.polymer.2006.01.093.

[25] Y. Fu, L.-T. Lim, Investigation of multiple-component diffusion through LLDPE film using an FTIR-ATR technique, Polym. Test. 31 (2012) 56–67. doi:10.1016/j.polymertesting.2011.08.015.

[26] D.T. Hallinan, Y.A. Elabd, Diffusion and Sorption of Methanol and Water in Nafion Using Time-Resolved Fourier Transform Infrared−Attenuated Total Reflectance Spectroscopy, J. Phys. Chem. B. 111 (2007) 13221–13230. doi:10.1021/jp075178n.

[27] Y.A. Elabd, E. Napadensky, J.M. Sloan, D.M. Crawford, C.W. Walker, Triblock copolymer

ionomer membranes Part I. Methanol and proton transport, J. Memb. Sci. 217 (2003) 227–242. doi:10.1016/s0376-7388(03)00127-3.

[28] Y.A. Elabd, M.G. Baschetti, T.A. Barbari, Time-Resolved Fourier Transform Infrared/Attenuated Total Reflection Spectroscopy for the Measurement of Molecular Diffusion in Polymers, J. Polym. Sci. Part B Polym. Phys. 41 (2003) 2794–2807.

[29] N.W. DeLuca, Y.A. Elabd, Nafion®/poly(vinyl alcohol) blends: Effect of composition and annealing temperature on transport properties, J. Memb. Sci. 282 (2006) 217–224. doi:10.1016/j.memsci.2006.05.025.

[30] G.A. Giffin, S. Lavina, G. Pace, V. Di Noto, Interplay between the Structure and Relaxations in Selemion AMV Hydroxide Conducting Membranes for AEMFC Applications, J. Phys. Chem. C. 116 (2012) 23965–23973. doi:10.1021/jp3094879.

[31] X.T. Le, T.H. Bui, P. Viel, T. Berthelot, S. Palacin, On the structure-properties relationship of the AMV anion exchange membrane, J. Memb. Sci. 340 (2009) 133–140. doi:10.1016/j.memsci.2009.05.025.

[32] E.L. Clark, M.R. Singh, Y. Kwon, A.T. Bell, Differential Electrochemical Mass Spectrometer Cell Design for Online Quantification of Products Produced during Electrochemical Reduction of CO2, Anal. Chem. 87 (2015) 8013–8020. doi:10.1021/acs.analchem.5b02080.

[33] M.R. Singh, Y. Kwon, Y. Lum, J.W. Ager, A.T. Bell, Hydrolysis of Electrolyte Cations Enhances the Electrochemical Reduction of CO2 over Ag and Cu, J. Am. Chem. Soc. 138 (2016) 13006–13012. doi:10.1021/jacs.6b07612.

[34] Y. Lum, Y. Kwon, P. Lobaccaro, L. Chen, E.L. Clark, A.T. Bell, et al., Trace Levels of Copper in Carbon Materials Show Significant Electrochemical CO2 Reduction Activity, ACS Catal. 6 (2016) 202–209. doi:10.1021/acscatal.5b02399.

[35] Beer, Bestimmung der Absorption des rothen Lichts in farbigen Flüssigkeiten, Ann. Der Phys. Und Chemie. 162 (1852) 78–88. doi:10.1002/andp.18521620505.

[36] H. Yasuda, A. Peterlin, C.K. Colton, K.A. Smith, E.W. Merrill, Permeability of Solutes through Hydrated Polymer Membranes. Part III. Theoretical Background for the Selectivity of Dialysis Membranes, Makromol. Chemie. 126 (1969) 177–186.

[37] G.M. Geise, B.D. Freeman, D.R. Paul, Characterization of a sulfonated pentablock copolymer for desalination applications, Polymer. 51 (2010) 5815–5822. doi:10.1016/j.polymer.2010.09.072.

[38] H. Wu, Q. Gong, D.H. Olson, J. Li, Commensurate Adsorption of Hydrocarbons and Alcohols in Microporous Metal Organic Frameworks, Chem. Rev. 112 (2012) 836–868. doi:10.1021/cr200216x.

[39] M. Soltanieh, S. Sahebdelfar, Interaction effects in multicomponent separation by reverse osmosis, J. Memb. Sci. 183 (2001) 15–27. doi:10.1016/S0376-7388(00)00554-8.

[40] D.C. Harris, Quantitative Chemical Analysis, Sixth Edit, W. H. Freeman and Company, New York, 2003.

Supporting Information for Multicomponent Transport of Alcohols in an Anion Exchange Membrane Measured by *In-Situ* ATR FTIR Spectroscopy

Blaine M. Carter,[1] Breanna M. Dobyns,[2] Bryan S. Beckingham,[2] and Daniel J. Miller[1]*

*Corresponding Author, Tel: +1 (510) 495-2353 E-mail: danieljmiller@lbl.gov

[1]Joint Center for Artificial Photosynthesis. Lawrence Berkeley National Laboratory, Berkeley, CA 97420, United States

[2]Department of Chemical Engineering, Auburn University, Auburn, AL 36849, United States

Table S1. Comparison of actual and measured concentrations in binary solutions of methanol and ethanol.

Actual Concentration (M)		**Measured Concentration (M)**			
Methanol	Ethanol	Methanol	Error (%)	Ethanol	Error (%)
0.05	0.05	0.0598	20	0.0575	15
0.10	0.10	0.1071	7	0.1035	3
0.15	0.15	0.1582	5	0.1555	4
0.075	0.125	0.0767	2	0.1256	0.5
0.125	0.075	0.1276	2	0.0757	1

Table S2. Comparison of actual and measured concentrations in binary solutions of methanol and *n*-propanol.

Actual Concentration (M)		**Measured Concentration (M)**			
Methanol	*n*-Propanol	Methanol	Error (%)	*n*-Propanol	Error (%)
0.05	0.05	0.0600	20	0.0496	1
0.10	0.10	0.1074	7	0.0972	3
0.15	0.15	0.1606	7	0.1516	1
0.075	0.125	0.0786	5	0.1210	3
0.125	0.075	0.1268	1	0.0627	16

Table S3. Comparison of actual and measured concentrations in binary solutions of ethanol and *n*-propanol.

Actual Concentration (M)		**Measured Concentration (M)**			
Ethanol	*n*-Propanol	Ethanol	Error (%)	*n*-Propanol	Error (%)
0.05	0.05	0.0570	14	0.0480	4
0.10	0.10	0.0986	1	0.0908	9
0.15	0.15	0.1542	3	0.1494	0.4
0.075	0.125	0.0753	0.4	0.1163	7
0.125	0.075	0.1250	0.01	0.0666	11

Table S4. Comparison of actual and measured concentrations in ternary solutions of methanol, ethanol, and *n*-propanol.

Actual Concentration (M)			**Measured Concentration (M)**					
Methanol	Ethanol	*n*-Propanol	Methanol	Error (%)	Ethanol	Error (%)	*n*-Propanol	Error (%)
0.05	0.05	0.05	0.0505	1	0.0504	1	0.0429	14
0.10	0.10	0.10	0.1047	5	0.1008	1	0.0928	7
0.15	0.15	0.15	0.1524	2	0.1516	1	0.1410	6